

***CARLETON UNIVERSITY
SPACECRAFT DESIGN PROJECT
2004 FINAL DESIGN REPORT***

Satellite Mission Analysis

FDR Reference Code: FDR-SAT-2004-3.2.A

Team/Group: Satellite Mission Analysis

Date of Submission: April 8th, 2004

COPY 1

Prepared by: Shawn Beaudette
Satellite Mission Analysis

Date: 6/04/2004

Checked by: Derrick Piontek
Command & Data Handling

Date: 7/04/2004

Abstract

This report details the analysis performed to determine the orbital parameters for the AEGIS satellite. The final orbit is a circular, sun-synchronous, dawn-dusk orbit at an altitude of 699 km. This orbit offers maximum access to sunlight, hot and cold measurements of targets, a high target revisit rate and minimal distortion.

The mapping and pointing budgets for the mission have been developed and are currently acceptable. The mapping and pointing budget indicate that it is possible to image as low as 45° and still maintain adequate results. The effect of launch injection errors on mission life was analyzed and the satellite will be designed to adequately account for them. Launch injection errors from the Pegasus launch vehicle are being used to estimate what can be expected from the AEGIS launch vehicle. A preliminary analysis of NASA STDN ground station availability during the early orbit phase has been performed. The analysis is based upon maximum access time with the ground stations as well as previous usage by the CSA.

Contents

1	Introduction	1
2	Orbital Mechanics	1
2.1	Classical Orbital Elements	1
2.2	Orbital Perturbations	3
2.2.1	Third-Body Perturbations	3
2.2.2	Perturbations Due to a Non-Spherical Earth	3
2.2.3	Atmospheric Drag	4
2.2.4	Solar Radiation	5
3	Design Requirements	5
4	Analysis	7
4.1	Satellite Tool Kit	7
4.2	Orbit Selection	7
4.2.1	Circular	7
4.2.2	Sun-Synchronous, Dawn-Dusk	7
4.2.3	Orbit Altitude	10
4.2.4	Minimum Elevation of 55 deg Requirement	14
4.2.5	Summary	16
4.3	Mapping and Pointing Errors	17
4.3.1	Sources of Pointing and Mapping Error	17
4.3.2	Mapping and Pointing Budget	18
4.4	Mission Life Analysis and Launch Injection Errors	21
4.5	Early Orbit Access Opportunities	23
5	Results	25
6	Conclusions	26
7	Future Work	26
	References	27
	Bibliography	28

Appendix A	Angular Relationship Calculation Spreadsheet	29
Appendix B	Mapping and Pointing Budget Calculation Spreadsheet	31
Appendix C	Injection Errors Calculation Spreadsheet	33
Appendix D	Lifetime due to Atmospheric Drag Sample Graph	35

List of Figures

2.1	Classical Orbital Elements [1]	2
4.1	Satellite at Latitude of 60° on March 21	9
4.2	Satellite at Latitude of 60° on June 21	9
4.3	Angular Relationships Between Satellite, Target and Earth Centre [5]	11
4.4	Satellite Ground Track After 2 Days	12
4.5	Satellite Ground Track After 7 Days	13
4.6	Satellite Coverage After 2 Days	15
4.7	Mapping Error as a Function of Elevation Angle	19
4.8	Pointing Error as a Function of Elevation Angle	20
4.9	Early Orbit Access Opportunities	24
D.1	Lifetime vs. Year of Launch for Ballistic Coefficient of 150 kg/m^2	36

List of Tables

4.1	Angular Relationships and Distortion Factor for 699 km Orbit	14
4.2	Typical Error Magnitudes, and Mapping and Pointing Error Equations	18
4.3	Pegasus Launch Injection Errors	22

Abbreviations

CCRS	Canadian Centre for Remote Sensing
CSA	Canadian Space Agency
CNES	Centre National d'Etudes Spaciales
DLR	Deutsche Forschungsanstalt fr Luft- und Raumfahrt
ESA	European Space Agency
HPOP	High Precision Orbit Propagator
INPE	Instituto Nacional de Pesquisas Espaciais
IR	InfraRed
LEO	Low Earth Orbit
LEOP	Launch and Early Orbit Phase
LTAN	Local Time of Ascending Node
NASA	National Aeronautics and Space Administration
NASDA	National Space Development Agency of Japan
NOAA	National Oceanic & Atmospheric Administration
RAAN	Right Ascension of the Ascending Node
STK	Satellite Tool Kit
STDN	Space-flight Tracking and Data Network
UdC	University of Chile
USAF	United States Air Force

Nomenclature

h	Altitude [km]
ω	Argument of Perigee [$^{\circ}$]
ρ	Atmospheric Density [kg/m ³]
ϕ	Azimuth Angle of Target Relative to Ground Track [$^{\circ}$]
C_D	Coefficient of Drag
A	Cross-Sectional Area [m ²]
A_S	Cross-Sectional Area Exposed to Sun [m ²]
D	Distance from Target [km]
λ	Earth Centre Angle [$^{\circ}$]
e	Eccentricity
ϵ	Elevation Angle [$^{\circ}$]
R_E	Equatorial Radius of the Earth [km]
i	Inclination [$^{\circ}$]
m	Mass of Satellite [kg]
η	Nadir Angle [$^{\circ}$]
n	Number of Orbits per Day
R_a	Radius of Apogee [km]
R_p	Radius of Perigee [km]
r	Reflection Factor
Ω	Right Ascension of Ascending Node [$^{\circ}$]
a	Semi-Major Axis [km]
b	Semi-Minor Axis [km]
ν	True Anomaly [$^{\circ}$]

1 Introduction

The primary task of the satellite mission analysis team is to select the optimum orbit which best enables the satellite and payload to perform their missions. The task is performed by first analyzing the mission, payload and satellite design requirements to determine if the mission is feasible. Providing the mission is feasible, trade-offs are performed in order to find a suitable orbit that meets the mission goals. This report includes a i) introduction to orbital mechanics, ii) description of the various design requirements, iii) the analysis performed to select the final orbit parameters, iv) the development of the mapping and pointing budget, v) an analysis of the effects of launch vehicle injection errors on the mission life, and vi) a preliminary analysis of ground station access for the early orbit phase.

2 Orbital Mechanics

The content of this report is almost entirely based on orbital mechanics. This section will attempt to provide some background on the subject, particularly the parameters that will be used to describe orbits in this report will be defined below. Although hopefully this section will be adequate to help the reader understand the rest of the report, it is encouraged that the reader refer to *Space Mission Analysis and Design* or the *STK Online Help* for clarification or further detail on orbital mechanics. The *STK Online Help* is invaluable when learning the STK software package which is used to compliment much of the analysis described in this report.

2.1 Classical Orbital Elements

From Kepler's first law of planetary motion, it is known that a satellite's orbit is an ellipse and the body it orbits is at one focus. Any Keplerian orbit can be completely described by six orbital elements, two to describe the size and shape, three to describe the orientation and one to describe the satellite location. In this report, the classical orbital elements will be used and it will be assumed that we are referring to an earth-orbiting satellite. These elements are: semi-major axis, eccentricity, inclination, right ascension of the ascending node, argument of perigee and true anomaly. It is important to note that a variety of orbital elements can be used to describe orbits; the classical system is just one of the more common. Figure 2.1 on the following page shows the classical orbital elements and a description of each of the elements follows.

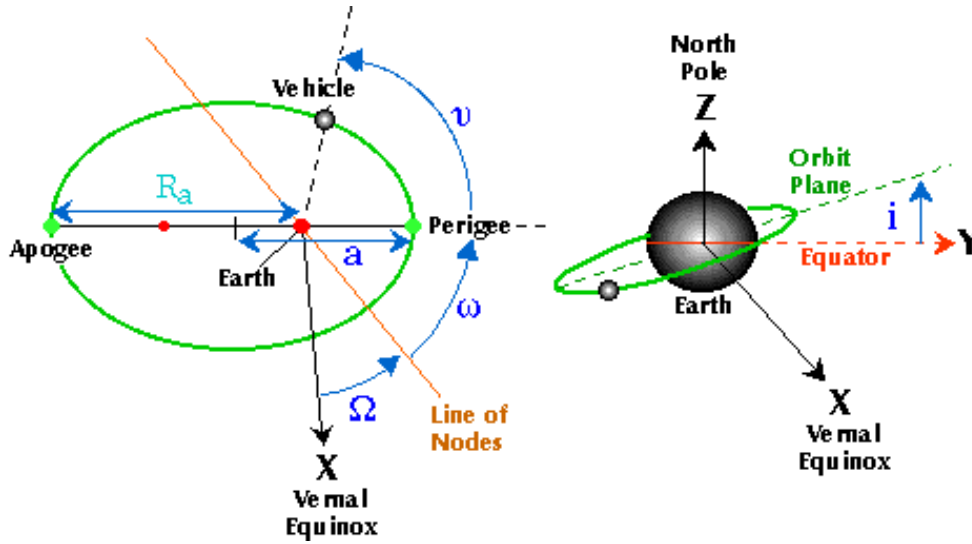


Figure 2.1: Classical Orbital Elements [1]

Semi-major Axis (a): The semi-major axis describes the size of the orbit. For a circular orbit, the semi-major axis is the radius of the earth plus the altitude (h) of the satellite. For elliptical orbits, the semi-major axis is half of the major axis diameter.

Eccentricity (e): The eccentricity describes the shape of the orbit ellipse. It is a measure of how circular an orbit is. It can be calculated as the distance from the centre of an ellipse to the focus divided by the semi-major axis. For a circular orbit, the eccentricity is 0.

Inclination (i): The inclination describes the orientation of the orbit. It is defined as the angle between the orbit plane and the equatorial plane.

Right Ascension of the Ascending Node (Ω): The Right Ascension of the Ascending Node (RAAN) describes the orientation of the satellite. It is the angle from the vernal equinox to the ascending node. The ascending node is the location where the satellite crosses the equatorial plane traveling from south to north.

Argument of Perigee (ω): The argument of perigee describes the orientation of the orbit. It is the angle between the ascending node and the eccentricity vector. The eccentricity vector points from the Earth's center to the perigee of the ellipse with a magnitude equal to the eccentricity. It is undefined for circular orbits.

True Anomaly (ν): The true anomaly describes the location of the satellite within the orbit. It is the angle between the eccentricity vector and the satellite measured in the direction of the satellite's motion.

2.2 Orbital Perturbations

The Keplerian orbital elements that will be selected in this report are osculating elements. Osculating elements describe the unperturbed (two-body) orbit that the satellite would follow if the outside perturbations were to cease instantaneously. There are a variety of effects that will cause these parameters to change during the lifetime of the satellite; as a result, the initial orbit parameters are defined with respect to an epoch. Some of the perturbing effects are described in the next section.

2.2.1 Third-Body Perturbations

The third-body perturbations are dominated by the gravitational forces of the Sun and the Moon. These forces cause small periodic variations in all the orbital elements but the RAAN and argument of perigee experience secular variations which are more important. The secular rates of change can be approximated as:

- Right ascension of the ascending node:

$$\dot{\Omega}_{MOON} = -0.00338(\cos i)/n \quad (1)$$

$$\dot{\Omega}_{SUN} = -0.00154(\cos i)/n \quad (2)$$

- Argument of Perigee:

$$\dot{\omega}_{MOON} = 0.00169(4 - 5 \sin^2 i)/n \quad (3)$$

$$\dot{\omega}_{SUN} = 0.00077(4 - 5 \sin^2 i)/n \quad (4)$$

where $\dot{\Omega}$ and $\dot{\omega}$ are in deg/day.

2.2.2 Perturbations Due to a Non-Spherical Earth

The Earth is often approximated as being spherical with a symmetric mass distribution. In reality the Earth has bulge at the equator and flattening at the poles. It is possible to model the geopotential of the earth using a matrix of coefficients. For example, the

common Goddard Earth model 10B is a 21x21 matrix of coefficients. In this report, we only consider the effects of J_2 zonal coefficient which accounts for the oblateness of the Earth. Similar to the third-body perturbations, the Earth's geopotential causes periodic variations in all orbital elements but these are again dominated by the secular variations in RAAN and argument of perigee due to the J_2 coefficient. These secular rates of change can be approximated as:

$$\dot{\Omega}_{J_2} = -2.06474 \times 10^{14} a^{-7/2} (\cos i) (1 - e^2)^{-2} \quad (5)$$

$$\dot{\omega}_{J_2} = 1.03237 \times 10^{14} a^{-7/2} (4 - 5 \sin^2 i) (1 - e^2)^{-2} \quad (6)$$

where $\dot{\Omega}$ and $\dot{\omega}$ are in deg/day. There are several sources that offer a more in depth analysis of the Earth's gravitational model. The Colorado Centre for Astrodynamics Research's website contains a detailed derivation for a 70x70 geopotential model [2].

2.2.3 Atmospheric Drag

Atmospheric drag is the principal non-gravitational force acting on a satellite and it only affects satellites in low-Earth orbit. Drag acts in the direction of opposite of the satellite's velocity resulting in a removal of energy from the orbit. This loss of energy results in the size of the orbit decreasing which then leads to a further increase in drag. Eventually the orbit becomes small enough that it reenters the Earth's atmosphere. The equation for the change in semi-major axis per revolution for circular orbits can be found below and further equations that govern the changes in orbital elements can be found in Chapter 6 of *Space Mission Analysis and Design* [3].

$$\Delta a_{rev} = -2\pi(C_D A/m)\rho a^2 \quad (7)$$

It is important to note that the atmospheric drag effects on a LEO satellite are heavily dependant on the time of launch. This is due to the 11 year solar cycle that causes the Earth's atmosphere to effectively swell up. An excellent discussion of atmospheric drag effects on a LEO satellite, which takes into account time of launch, is available from the Canadian Aeronautical and Space Institute ASTRO 2002 Conference entitled *Effects of Launch Injection Errors and Atmospheric Drag on SCISAT-1 Orbit Degradation* [4]. The paper demonstrates the varying atmospheric drag effects due to changes in altitude, ballistic coefficient and year of launch.

2.2.4 Solar Radiation

Solar radiation pressure is an effect that is strongest on satellites with large area to mass ratios. It results in periodic variations in all orbital elements. The magnitude of the acceleration due to solar radiation pressure in m/s^2 is approximately:

$$a_R \approx -4.5 \times 10^{-6}(1 + r)A_S/m \quad (8)$$

Solar radiation pressure is primarily a concern with geosynchronous satellites. The effects on a LEO microsatellite will be negligible.

3 Design Requirements

The initial design requirements for the mission came primarily from the payload although there were also requirements from the power subsystem and the launch vehicle. The payload mission goals are soil moisture mapping and silica detection. Details concerning the payload mission can be found in TPS-SAT-2004-3.1.A and TPS-SAT-2004-3.1.B. The requirements outlined below pertain to these two goals.

Payload Subsystem Requirements:

- High revisit rate of desired target
- Hot and cold measurements of each target
- Global coverage, priority given to Canada
- Maximize resolution (at least 50 m attainable)
- Three year mission life

Power Subsystem Requirements:

- Maximize access to sunlight

Launch Vehicle Requirements:

- Maximum altitude of 800 km
- Maximum inclination of 98.61 deg

The payload requirements relate primarily to soil moisture mapping. To perform the mission, the payload requires a hot and cold (day and night) measurement of a single target to determine the moisture content of that target. The payload will then revisit that target at the same time of day on subsequent passes to determine short term and long term trends in the moisture content of the target. The payload team estimates that three years is required to adequately determine long term trends.

Global coverage is preferred for the mission. In the case that global coverage is not possible or if there are conflicting areas of interest; priority will be given to Canadian targets and Canadian clients. This is primarily due to the fact that AEGIS is a Canadian university project which would likely obtain funding from Canadian industry and/or government grant.

Current technologies are able to obtain IR imaging at 60 m resolution. The mission must be able to obtain a resolution that is better or at least as good as current technology. The current goal is to obtain 50 m resolution in order to be a leader in the field.

The payload team gave no direct requirements for the secondary mission of silica detection. There is some question as to whether the detection of silica can be filtered from the acquired signal. The primary concern is that the received signal will be too noisy during any daytime measurements. More research is required to determine if this is accurate. Should it prove true, silica mapping can still be done but the data will only be obtainable from the nighttime measurements.

The power subsystem requirements are due to the fact that the team was having great difficulty meeting the power budget requirements. This difficulty lead to the maximum access to sunlight requirement. However, in the final satellite bus design it was still required to implement a deployable solar array system to meet the bus and payload power requirements.

The launch vehicle being design by the AEGIS team set a maximum altitude of 800 km and a maximum inclination of 98.6° . The launch vehicle team decided that this altitude would allow them to accommodate most LEO microsatellite missions. Therefore, the mission analysis team was limited to this altitude in order to integrate the satellite and launch vehicle into one system.

Another payload requirement was added after the initial analysis was completed. Due to the nature of the imaging the payload will be doing, the minimum elevation angle for imaging was required to be 55° . This requirement was provided to the payload team by Dr. Zwick at MacDonald, Dettwiller and Associates Ltd. The impact of this additional requirement will be discussed in the analysis section.

4 Analysis

4.1 Satellite Tool Kit

Satellite Tool Kit (STK) is recognized as the leading commercial off-the-shelf analysis tool for the aerospace industry. Unless otherwise stated, all orbital calculations in the analysis section of this report have been performed through hand/spreadsheet calculations and verified using STK v4.3. The simulations were performed using the J4Perturbation orbit propagator in order to reduce simulation time. This propagator does not include third-body, solar radiation or atmospheric drag perturbing effects. It also does not include geopotential perturbations above those of J4. The J4Perturbation orbit propagator offers a reasonable first iteration estimate of the orbit's behavior. Future iterations may wish to use the High Precision Orbit Propagator (HPOP) which includes the perturbing effects mentioned above.

4.2 Orbit Selection

The orbit selection is based on the initial design requirements. The analysis for the orbit selection is simplified by the fact that the orbit requirements of the power subsystem and launch vehicle correspond very well with the payload requirements. Thus, very few trade-offs between the subsystems had to be performed.

4.2.1 Circular

AEGIS is an earth-observation satellite that aims to be able to image globally. It was determined that an elliptical orbit offered no advantages. Therefore, it was decided to use a circular orbit ($e = 0$).

4.2.2 Sun-Synchronous, Dawn-Dusk

The mass of AEGIS is budgeted at 45 kg and the volume is 0.125 m³. AEGIS has very high power requirements for its size, details of these requirements can be found in FDR-SAT-2004-3.5.A and FDR-INT-2004-1.D. Through preliminary analysis, the power subsystem team determined that in order to generate enough power for all the subsystems, it required a sun-synchronous, dawn-dusk orbit.

A sun-synchronous orbit is one which has a precession rate ($\dot{\Omega}$) such that it maintains an almost constant orientation with respect to the sun. This requires the precession rate of the orbit to match the orbit of the earth around the sun which is 360°/365.25 days or

0.9856°/day. By using equation (5), semi-major axes and corresponding inclinations can be determined that result in a sun-synchronous orbit.

Dawn-dusk is an orientation where the orbit plane has its Local Time of Ascending Node (LTAN) at 6:00am; essentially the orbit plane “faces” the sun. If the satellite is placed in a sun-synchronous orbit with a dawn-dusk orientation, this will maximize its access to sunlight (the satellite will only experience eclipses for approximately 3 months of the year and the eclipse durations will generally be shorter than other orbits), thus allowing it to generate the maximum amount of power from its solar cells.

From the perspective of the microbolometer payload, a sun-synchronous, dawn-dusk orbit is also beneficial. The payload requires hot and cold measurements of targets. On average, the ground will be at its coldest just prior to dawn (6:00am local time) because the soil is continually cooling so long as the sun is not in contact with it. However, it is estimated that the ground is at its hottest during mid-afternoon (approximately 3:00pm local time). The payload wants to measure a target at the same local time each day which requires a sun-synchronous orbit. The payload also wants to maximize the difference in ground temperature between the hot and cold measurements. A 3:00am-3:00pm orbit orientation would acquire the hottest possible measurement at 3:00pm but not coldest. A 6:00am-6:00pm (dawn-dusk) orbit would acquire the coldest possible measurement at 6:00am but not the hottest. In order to make the selection, it was reasonably assumed that the difference between ground temperatures in the two orbits would be approximately the same. Therefore, due to the large advantage that is gained in terms of power, it was chosen to use a 6:00am-6:00pm (dawn-dusk) orientation.

In a dawn-dusk orientation, the satellite will be traveling above the terminator line that separates night and day. However, a problem occurs at high latitudes during summer and winter when the days or nights become longer due to the 23.5° solar declination. The problem is illustrated using Figure 4.1 and Figure 4.2 on the next page.

In Figure 4.1, a satellite is shown on March 21 at a latitude of 60°. The satellite is above ground that has yet to see any sunlight, here the payload would take a cold measurement just prior to dawn. In Figure 4.2, the satellite is shown on June 21 at a latitude of 60°. In this case, the satellite would be taking a cold measurement on ground that was determined to have been in contact with sunlight for approximately 2 hours. Much work was done by Jesse Klostranec and the payload team to determine what effect this might have on the image data. It was determined that the short length of time combined with the low elevation angle of the sun would result in minimal change in ground temperature and the image data would maintain an acceptable level of quality.

The decision to launch into a dawn-dusk sun-synchronous orbit also affects the mission life requirements. The payload requires a mission life of three years. As mentioned in Section 1.2, several effects can perturb the satellite away from its nominal orbit. Specifically, the

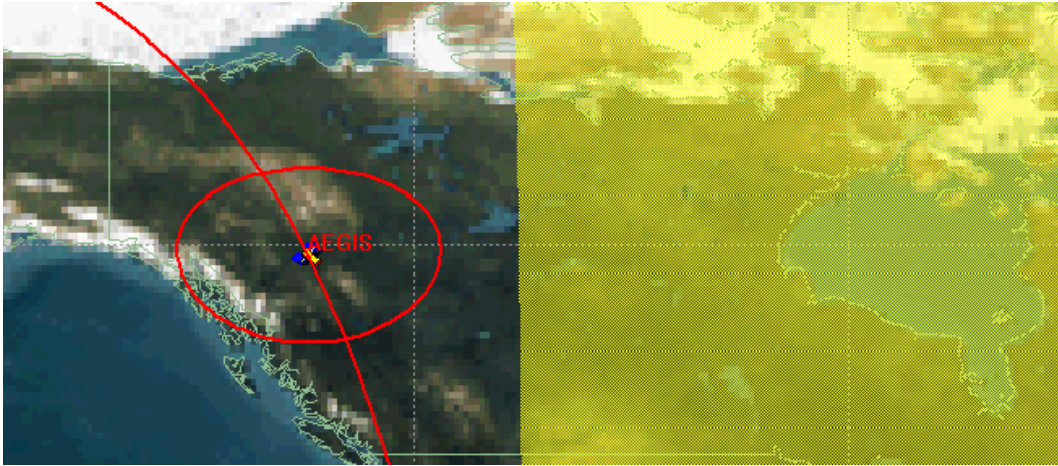


Figure 4.1: Satellite at Latitude of 60° on March 21

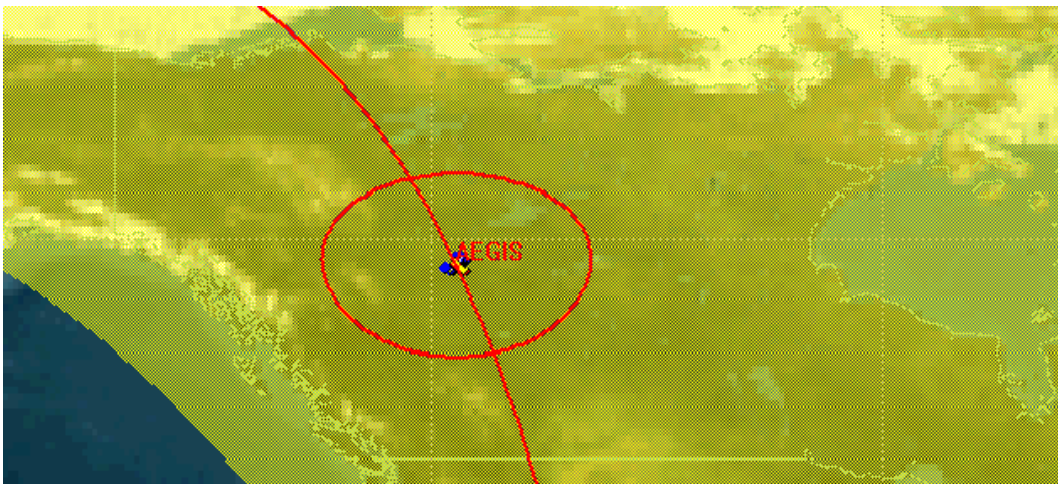


Figure 4.2: Satellite at Latitude of 60° on June 21

satellite will drift away from a dawn-dusk orientation if the precession rate is not $0.9856^\circ/\text{day}$, resulting in reduced access to sunlight. Although it is expected that the perturbation effects will be minimal at our nominal orbit, there are also launch vehicle injection errors that need to be considered. This will be covered in detail in Section 4.3.

4.2.3 Orbit Altitude

The size of the orbit affects the largest number of design requirements. Since we will be using payload and launch vehicle requirements to determine the size of the orbit, this section will use altitude as the orbit size parameter. Referring back to the classical orbital elements, for a circular orbit, the altitude is the semi-major axis less the Earth's radius.

The orbit altitude will affect the target revisit rate, the resolution, the coverage area and the mission life. A lower limit of 500 km is placed on the altitude, below 500 km the orbit life is very short due to atmospheric drag. An upper limit of 800 km is placed on the satellite by the launch vehicle capabilities. This upper limit is also desirable for the payload subsystem due to the decrease in resolution as altitude increases.

The payload team placed highest priority on the target revisit rate requirement. Ideally, the payload would like to be able to image any location, twice each day (once for a hot measurement and once for a cold measurement). However this is impossible because it would either require a very large roll manoeuvre for global coverage which results in very large distortions or it would require very high altitudes outside the 500-800 km envelope.

Figure 4.3 on the following page shows the geometrical relationships of the earth centre angle (λ), the elevation angle (ϵ), the altitude (H) and distance from target (D).

A simple spreadsheet was set up to calculate the resulting roll manoeuvre at the equator to obtain global coverage for the desired altitude and revisit rate. The spreadsheet uses the rotation rate of the earth relative to the orbit plane to determine the difference in degrees between the ascending nodes. Thus, for a given revisit rate and altitude, the maximum earth centre angle can be determined. Through simple geometry, the earth centre angle and altitude can be used to calculate the maximum roll angle at the equator required to obtain global coverage and the corresponding elevation angle. The spreadsheet can be adjusted to a new revisit rate or altitude by adding or removing additional passes as needed. For example, an altitude of 699 km and revisit rate of 2 days results in 30 passes. Varying altitude and revisit rate will change the number of passes and the spreadsheet will need to be adjusted for that. The spreadsheet is attached as Appendix A.

The distortion factor is also calculated in the spreadsheet. The distortion factor is used to calculate the resolution at any elevation. The distortion factor is calculated as:

$$\text{Distortion Factor} = \frac{1}{\sin \epsilon} \quad (9)$$

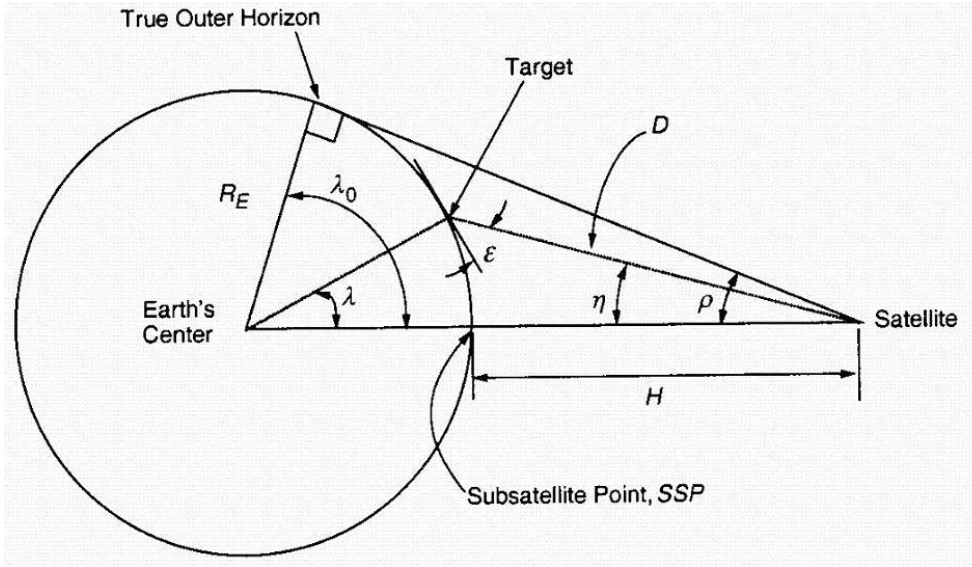


Figure 4.3: Angular Relationships Between Satellite, Target and Earth Centre [5]

The resolution at any elevation can then be calculated as:

$$\text{Resolution}_\epsilon = (\text{Distortion Factor}) \times (\text{Resolution at Nadir}) \quad (10)$$

It was determined that the optimum altitude is 699 km. For a sun-synchronous orbit, the inclination must then be 98.19° . This altitude is optimum because it was thought to have adequate roll requirements for a two day period but allows for a significant improvement in roll requirements for a seven day period. Figure 4.4 on the next page shows a typical ground track of the 699 km orbit over 2 days and Figure 4.5 on page 13 shows a ground track over 7 days. As can be seen in Figure 4.5, over 7 days the ground tracks are very close together requiring a much smaller roll angle to obtain global coverage. At this altitude, the satellite can acquire a day and night measurement of any location in a two day period at a maximum roll angle of approximately 46° and it can acquire a day and night measurement of any location in a seven day period at a maximum roll angle of 19.7° .

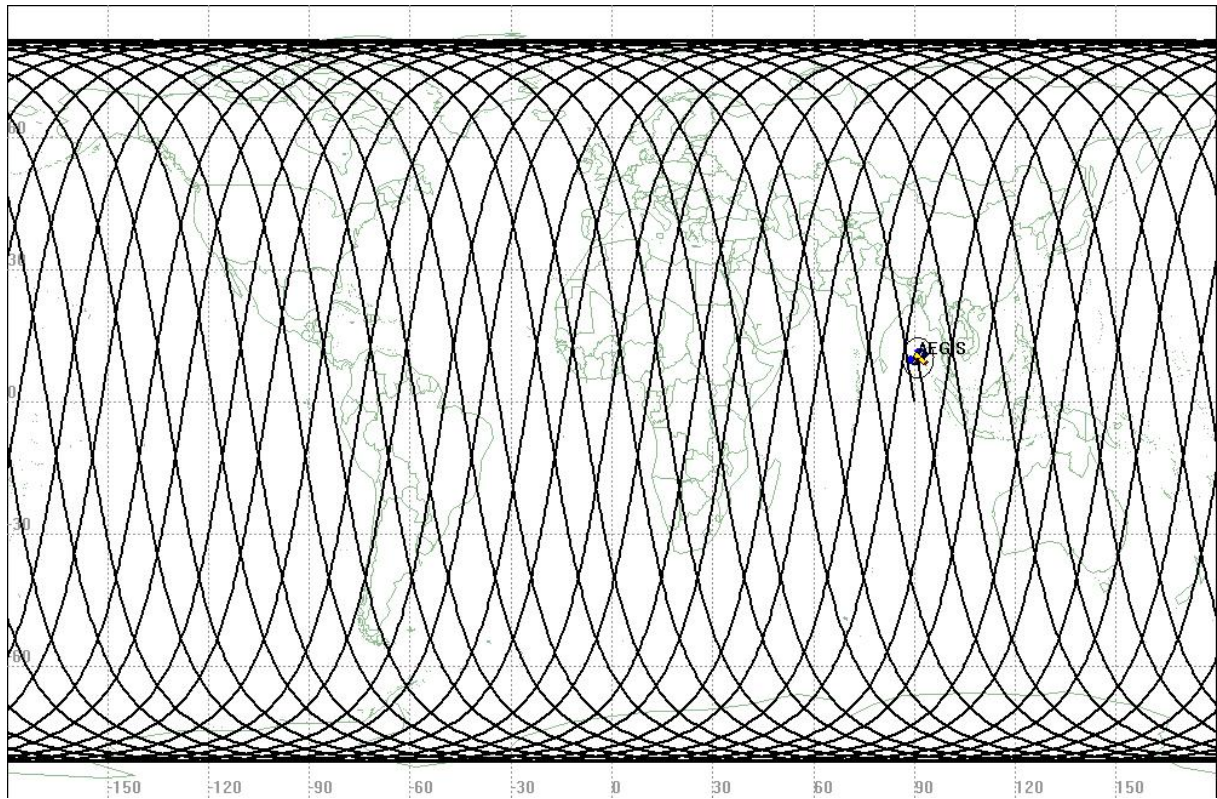


Figure 4.4: Satellite Ground Track After 2 Days

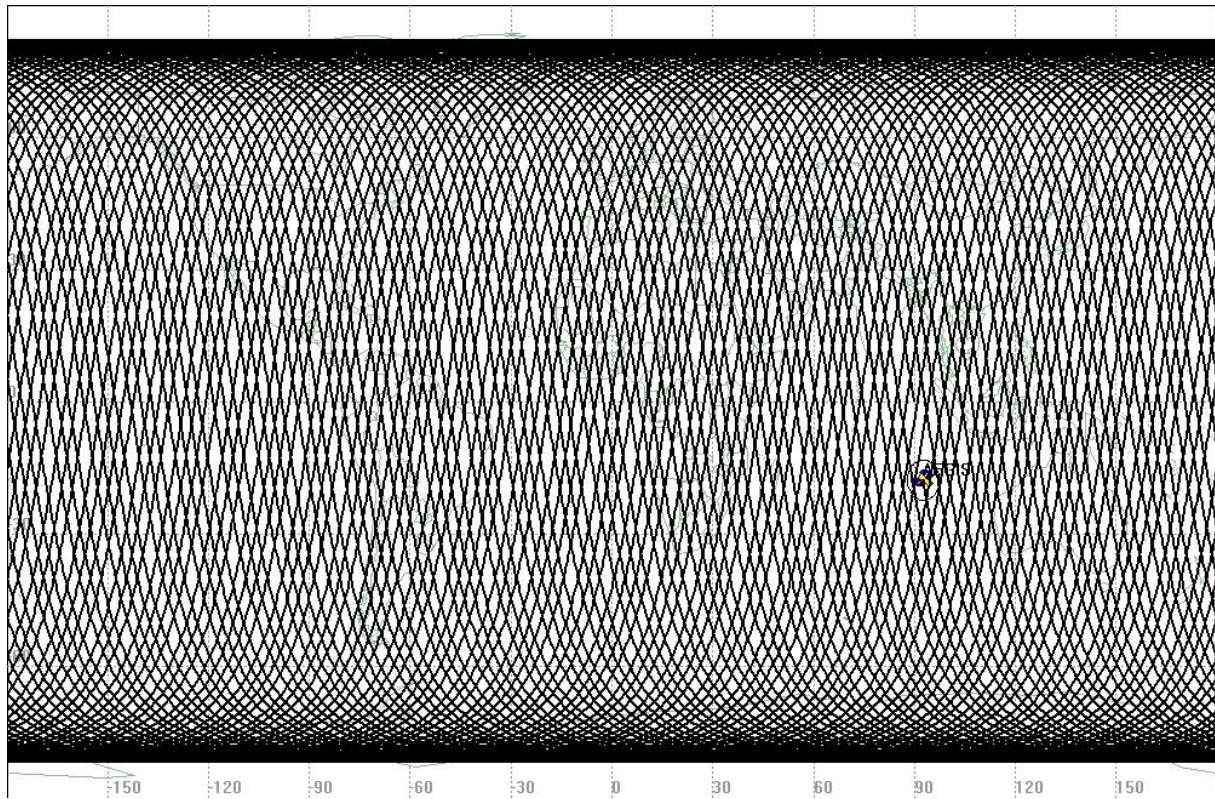


Figure 4.5: Satellite Ground Track After 7 Days

This scenario is beneficial because it is known that the payload will be imaging the same target for several passes for soil moisture mapping. Therefore, images at various roll angles and distortions will be acquired. Since it is known that the same target is being imaged, software on the ground can be used to “clean up” the low resolution distorted images using the high resolution images.

A summary of the roll angle requirements, corresponding elevation angles and distortion factors for the 699 km orbit is located in Table 4.1. The table includes both the results for a 2 day period and a 7 day period.

Period	Max Roll Angle	Minimum Elevation Angle	Distortion Factor
2 days	46.0 °	33.0 °	1.68
7 days	19.7 °	67.8 °	1.08

Table 4.1: Angular Relationships and Distortion Factor for 699 km Orbit

4.2.4 Minimum Elevation of 55 deg Requirement

As mentioned in the design requirements, after the completion of the orbit selection as outlined above, a new design requirement was added. The rule of thumb for IR imaging is not to image at elevation angles less than 55°. Originally it was desired to be able to image anywhere in the world in a two day period. This is no longer possible, because the current design results in elevation angles of 33°. However, it was determined that this does not invalidate the above analysis.

Through simulation it was found that at an altitude of 699 km and minimum imaging elevation of 55°, it is still possible to image anywhere in Canada in a two day period. This is due to the fact that at higher latitudes the ground tracks are closer together. This is illustrated in Figure 4.6 on the following page. Figure 4.6 shows the descending tracks of the satellite overlayed with the coverage to an elevation of 55° for a typical 2 day interval. In any 2 day interval, most of Canada can be imaged and as the latitude is decreased, gaps in the coverage appear. However, it should be noted that the gaps will not occur over the same locations in each 2 day interval. This allows us to obtain the desired coverage in Canada which is the priority area and to obtain adequate coverage at lower latitudes. The estimated coverage at the equator is that for any given target at 0 latitude, the payload would be able to acquire a minimum of 6 measurements over the course of 10 days (Ideally, the payload would have acquired 10 measurements).

The requirement of imaging at a minimum elevation angle of 55° was included late in the design and at the time it was undesirable to change the orbit due to the ripple effect it would have on the other subsystems. It was decided to accept the resulting coverage as opposed

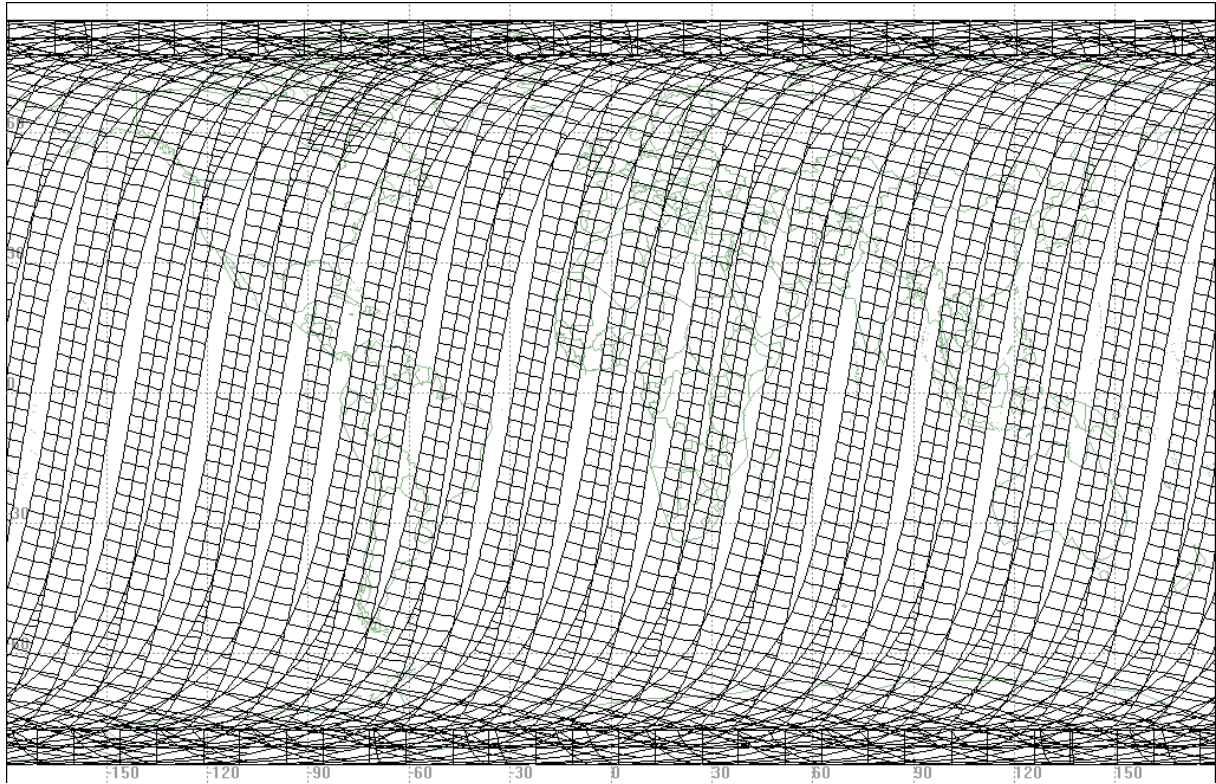


Figure 4.6: Satellite Coverage After 2 Days

to fine-tuning the orbit parameters to optimize it. An improvement in coverage would most likely require an increase in altitude to reduce the size of the gaps. However, a significant improvement may require a large increase in altitude which would be unfeasible. This issue should be explored in future iterations to ensure the best possible coverage. Additionally, a full understanding of the 55° elevation requirement would be beneficial. It is unclear whether this requirement will still hold true using the most recent technology.

4.2.5 Summary

The orbit design has been completed and the summary of the results is as follows:

- Circular orbit
- Sun-synchronous, dawn-dusk (LTAN = 6:00am)
- Altitude = 699 km
- Inclination = 98.19°

In terms of the classical orbital elements (Epoch = June 1 2003 00:00:00 UTC):

- Semi-major axis = 7077.1 km
- Eccentricity = 0
- Inclination = 98.19°
- RAAN = 339°
- Argument of perigee = N/A (circular orbit)
- True anomaly = 259° (determined by the launch vehicle team)

Through simulation it was determined that the eclipse season is approximately 3 months, starting in early November and ending in late January. The maximum duration of eclipse in this period is 1198 seconds (approximately 20 minutes).

At the minimum elevation angle for imaging of 55° , the satellite will be capable of acquiring day and night images of any location in Canada in a two day period and still acquire adequate coverage at the equator. The maximum distortion factor at 55° elevation is 1.22 and the roll required is approximately 31° .

4.3 Mapping and Pointing Errors

Any spacecraft performing earth-observation requires a pointing and mapping budget. Pointing refers to orienting the spacecraft instrument to a target having a specific geographic location. Mapping is the determination of the geographic location of the look point of the spacecraft instrument. A budget will list all sources of pointing and mapping errors and their contributions to the overall accuracies.

4.3.1 Sources of Pointing and Mapping Error

The following is a list of sources of pointing and mapping errors:

Spacecraft Position Errors:

- In-track(ΔI): Displacement along the spacecraft's velocity vector
- Cross-track (ΔC): Displacement normal to the spacecraft's orbit plane
- Radial (ΔR_S): Displacement toward the center of the Earth (nadir)

Sensing Axis Orientation Errors:

- Elevation ($\Delta \eta$): Error in angle from nadir to sensing axis
- Azimuth ($\Delta \phi$): Error in rotation of the sensing axis about nadir

Other Errors:

- Target Altitude (ΔR_T): Uncertainty in the altitude of the observed object
- Clock Error (ΔT): Uncertainty in the real observation time

Table 4.2 on the next page contains the error magnitudes and the equations used to calculate the mapping and pointing budget. The error magnitudes for nadir angle and azimuth angle are 0.1° and were obtained from the Attitude Determination and Control team as the accuracies provided from the earth sensors. The spacecraft position error magnitudes as well as target altitude error and clock error magnitudes are typical values that were obtained from *Space Mission Analysis and Design* [6].

There are many equations in Table 4.2. A description and derivation of each would be too

detailed for this report but all the variables are defined in the Nomenclature and illustrated in Figure 4.3 on page 11. The δX terms in each equation are the error magnitudes. For further information see Reference 6. The principles behind the mapping and pointing errors are of more interest. The errors in mapping are heavily dependant on how close the satellite is imaging to the horizon. If a satellite images only at nadir, it will have excellent mapping errors and resolution but very poor coverage. If a satellite images at the horizon, it will have excellent coverage but the mapping errors will be huge (several hundred kilometres) and resolution also decreases due to distortion (see section 4.2.3). The mapping and pointing budgets allow the operators to judge how close to the horizon, the satellite is able to image while still maintaining adequate mapping and pointing accuracies.

Error Source	Typical Error Magnitude	Mapping Error (km)	Pointing Error (rad)
Azimuth	0.06°	$\Delta\phi D \sin \eta$	$\Delta\phi \sin \eta$
Elevation	0.03°	$\Delta\eta D / \sin \epsilon$	$\Delta\eta$
In-Track	0.2 km	$\Delta I (R_E / (R_E + h)) \cos H^{(1)}$	$(\Delta I / D) \sin Y_l^{(2)}$
Cross-Track	0.2 km	$\Delta C (R_E / (R_E + h)) \cos G^{(3)}$	$(\Delta C / D) \sin Y_C^{(4)}$
Radial	0.1 km	$\Delta R_S \sin \eta / \sin \epsilon$	$(\Delta R_S / D) \sin \eta$
Target Altitude	1 km	$\Delta R_T / \tan \epsilon$	-
Clock Error	0.5 sec	$\Delta T V_e \cos(lat)^{(5)}$	$\Delta T (V_e / D) \cos(lat) \sin J^{(6)}$

Notes:

- (1) $\sin H = \sin \lambda \sin \phi$.
- (2) $\sin G = \sin \lambda \cos \phi$.
- (3) $\cos Y_l = \cos \phi \sin \eta$.
- (4) $\cos Y_C = \sin \phi \sin \eta$.
- (5) $V_e = 464 \text{ m/s}$ (Earth rotational velocity at the equator).
- (6) $\cos J = \cos \phi_E \cos \epsilon$, where $\phi_E = \text{azimuth relative to east}$.

Table 4.2: Typical Error Magnitudes, and Mapping and Pointing Error Equations

4.3.2 Mapping and Pointing Budget

A spreadsheet is attached as Appendix B which shows the values calculated for the mapping and pointing budget. Figure 4.6 on page 15 is a plot of the mapping budget and Figure 4.7 on the following page is a plot of the pointing budget.

It was already determined that to acquire an adequate image quality, the minimum elevation angle for imaging is 55° . Therefore it is necessary that adequate mapping and pointing at that elevation can be obtained as well. From Figure 4.8, it can be seen that the

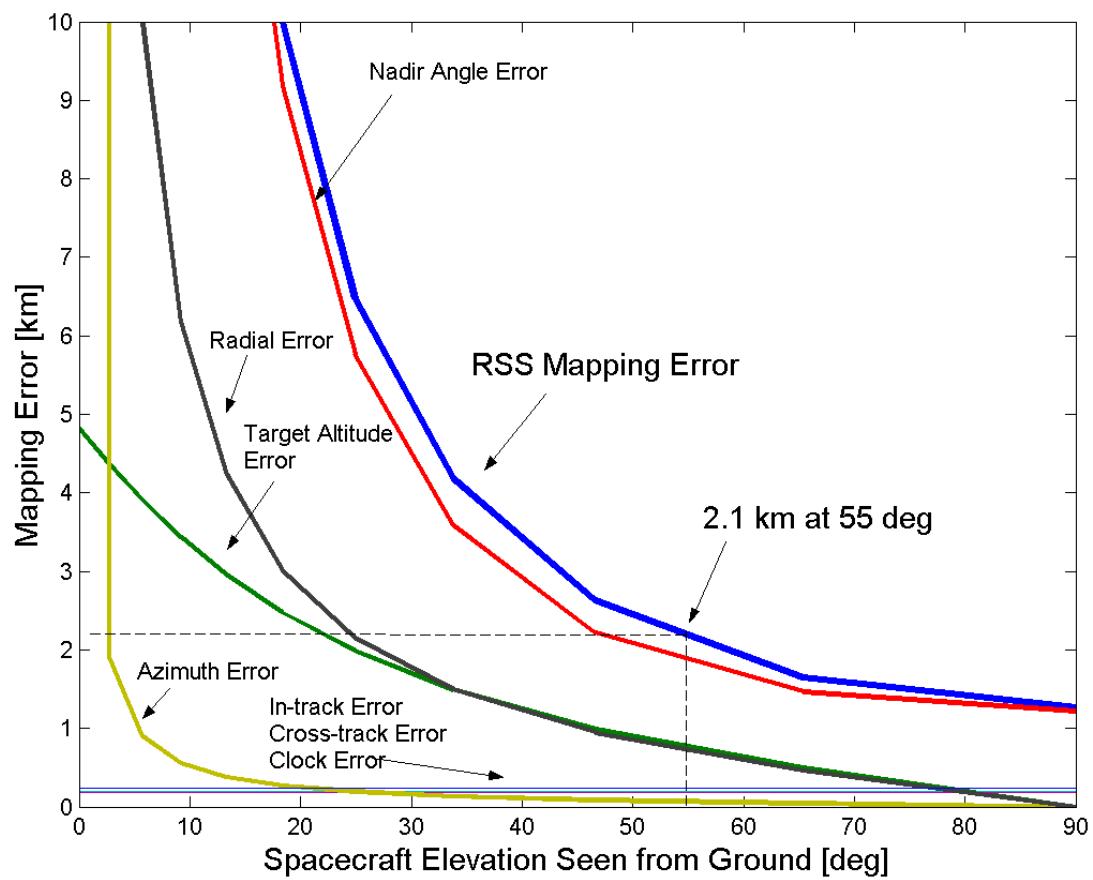


Figure 4.7: Mapping Error as a Function of Elevation Angle

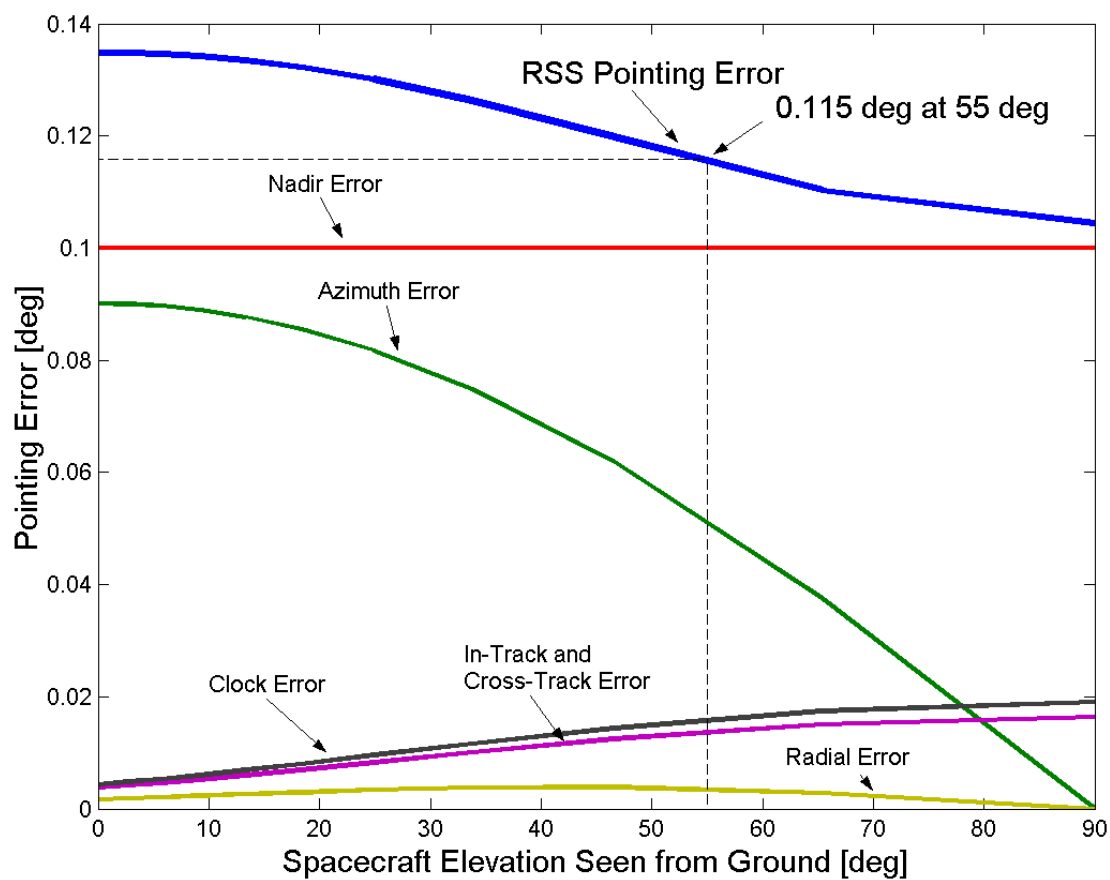


Figure 4.8: Pointing Error as a Function of Elevation Angle

mapping error is dominated by the nadir angle error. This implies that to see an improvement in the mapping error it would necessitate an improvement in the attitude determination subsystem, such as the inclusion of star sensors. An improvement like this would drive the cost of the mission up and is unfeasible. However, at an elevation of 55° , the mapping error is 2.1 km. It was determined that for the AEGIS mission, this mapping accuracy would be adequate and no improvement in attitude determination is needed. In Figure 4.8, a similar situation occurs where the pointing error is once again dominated by the nadir angle error. The same situation applies where an improved attitude determination system would be required to improve the result. However, again it was determined that a pointing accuracy of 0.115° at an elevation of 55° was adequate for the AEGIS mission.

It should also be noted that the mapping and pointing budgets are adequate at elevation angles as low as 40° where mapping and pointing errors of approximately 3 km and 1.2° occur respectively. Therefore, if the IR imaging could be performed at elevation angles less than 55° with satisfactory image quality; better coverage could be attained while still maintaining adequate mapping and pointing accuracies.

4.4 Mission Life Analysis and Launch Injection Errors

As mentioned in Section 4.1, a sun-synchronous, dawn-dusk orbit limits the mission life. This is because any perturbations will change the orbital elements resulting in a change from the nominal precession rate of $0.9856^\circ/\text{day}$ and without any way to compensate for these effects, the satellite will drift away from its dawn-dusk orientation. Fortunately, the orbit is at an altitude where the secular variations will have minimal effect. At 699 km, we are adequately high that atmospheric drag will have minimal effect during the three year mission life (this can be justified from a graph from Reference 4 which has been attached as Appendix D). Additionally, a lifetime estimate in the nominal orbit was performed using the lifetime analysis tool in STK to corroborate this assumption. The lifetime until de-orbit was calculated to be 110 years. We are adequately low that the gravitational effects of the sun and moon will be negligible. We will also assume that AEGIS will have a relatively high mass to area ratio so that solar radiation pressure will be negligible as well. As a result, the mission life of the satellite will be dominated by the accuracy of the launch vehicle.

Since there is no historical data for the AEGIS launch vehicle, it is unknown what the launch injection errors will be. For this analysis, the 1-sigma and 3-sigma launch injection errors for the Pegasus launch vehicle are used because the Pegasus has been determined to be the most similar to the AEGIS launch vehicle. Table 4.3 on the next page shows the 1-sigma and 3-sigma errors for the Pegasus as given in the *Pegasus User's Guide*[7].

The analysis is performed by applying the injection errors to the nominal orbit parameters and then using equation (5) to calculate the new precession rate. The difference between

	Insertion Apse	Non-Insertion Apse	Inclination
1-sigma	± 5 km	± 30 km	$\pm 0.05^\circ$
3-sigma	± 19 km	± 90 km	$\pm 0.15^\circ$

Table 4.3: Pegasus Launch Injection Errors

this precession rate and the nominal precession rate will be the rate at which the orbit will drift away from the dawn-dusk orientation. From the drift rate, the total error in RAAN after 3 years can be calculated. Appendix C contains the spreadsheet illustrating these calculations, verified using STK.

It was found that the worst case 1-sigma had drifted 16.9° after 3 years and the worst case 3-sigma had drifted 49.7° after 3 years. The power subsystem required a design point before it was possible to do a proper statistical analysis. It was decided that designing for a worst case 1-sigma was both feasible and conservative. In the future, it is recommended that a proper statistical analysis be performed in case the power subsystem is being over-designed due to a conservative estimate.

Currently, the satellite's power subsystem will be designed such that a three year mission can be attained provided the drift error in three years is less than 17° . In this worst case condition, the satellite would experience an eclipse season of nine months in its third year with a maximum eclipse duration of 1520 seconds (approximately 25.2 minutes). It is still necessary to analyze the cases where the drift error is greater than 17° in order to determine what mission life can be attained should one of those cases occur.

This analysis found that the drift rate in the positive and negative directions are not equal for equally likely events. Therefore it would be beneficial to move the local time of ascending node of the initial orbit such that the total drift error in the positive and negative direction with respect to 6:00am are equal. This requires moving the ascending node to approximately 6:05am, resulting in a new initial RAAN of 340° .

At the time this analysis was performed, it was decided to neglect atmospheric drag effects. This is a valid assumption in the nominal orbit; however, when applying negative injection errors, the orbit altitude is decreased. In the 1-sigma cases, the orbit will still be sufficiently high that the results will not dramatically change. Under 3-sigma cases, the altitude can be decreased to the low 600km range. In these cases, atmospheric drag may begin to have a more significant effect. Therefore, in the future work, it should be included to ensure the accuracy of the analysis.

4.5 Early Orbit Access Opportunities

Frequent communications with the satellite is highly desirable during Launch and Early Orbit Phase (LEOP). It was assumed that the AEGIS mission would primarily use the CCRS and CSA ground stations, however during the first few orbits NASA STDN compliant ground stations are often used by CSA satellites for communications during the early orbit phase. It is unknown which ground stations would be available for use at this time, however it was possible to determine a list of ideal ground stations based on the first five orbits of the AEGIS satellite. Figure 4.9 shows the locations and names of each of the selected ground stations. Ground station selection is based upon maximum access time, and knowledge of previous use by CSA for early orbit phases. This figure only includes a few of the possible ground stations, there are several dozen that could be used should they be unavailable. The ground stations (and their organization) selected are:

- American Samoa (NOAA)
- Canberra (NASA)
- Hickam Air Force Base (USAF)
- Liberville (DLR)
- Maspalomas (ESA)
- Natal (INPE)
- Perth (ESA)
- South Pacific French Kerguelen (CNES)
- St. Hubert (CSA)
- Santiago (UdC)
- Saskatoon (CSA)
- Thule Air Force Base (USAF)
- Tokyo (NASDA)

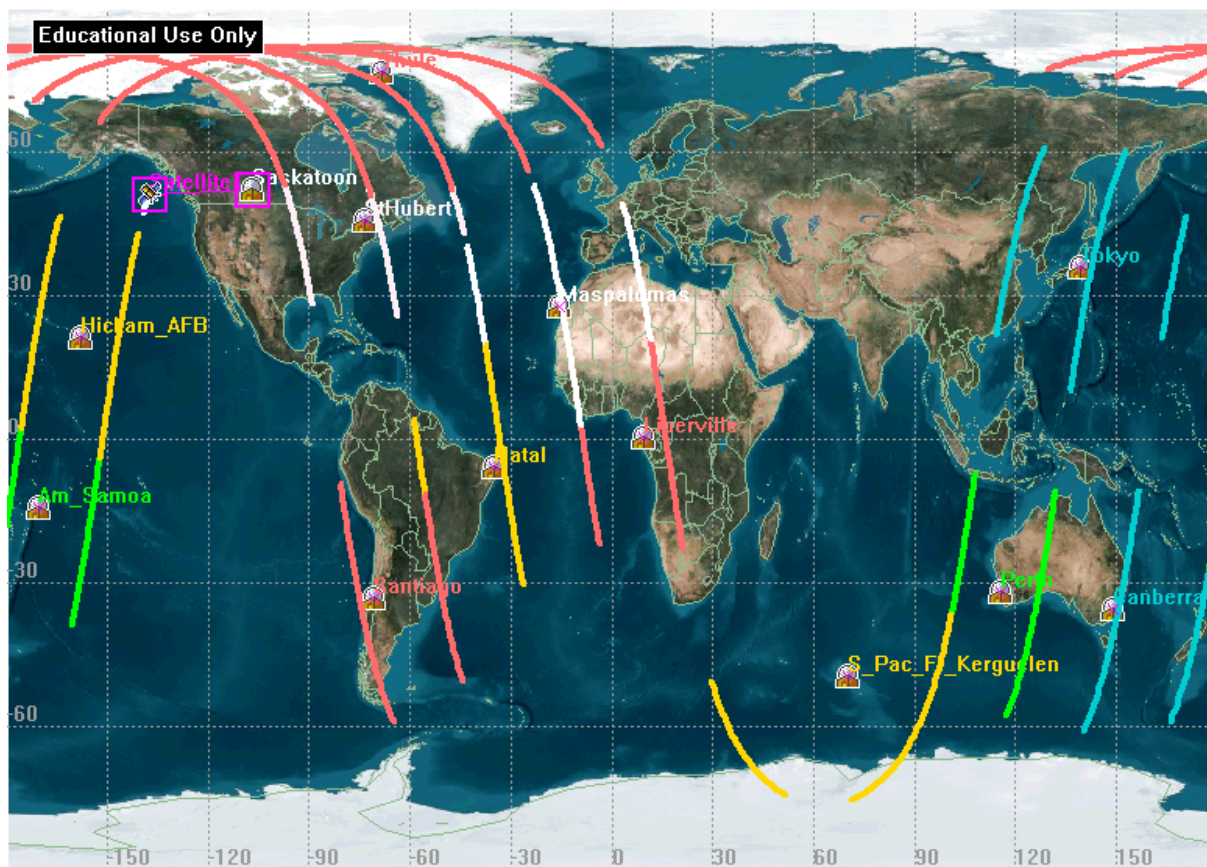


Figure 4.9: Early Orbit Access Opportunities

5 Results

The classical orbital elements that describe the selected orbit are listed below:

- Epoch = June 1, 2003, 00:00:00 UTC
- Semi-major axis = 7077.1 km
- Eccentricity = 0
- Inclination = 98.19°
- Right Ascension of the Ascending Node = 340°
- Argument of Perigee = N/A (circular orbit)
- True Anomaly = 259°

The mapping and pointing budgets are completed using error magnitude inputs from the attitude control and determination subsystem and typical values found in *Space Mission Analysis and Design*. The analysis for the launch injection errors and mission life is near completion using Pegasus XL errors. Further iterations needs to be done which use a more complete propagator such as HPOP. The current analysis demonstrates that the mission life is feasible but the satellite team may be over-designing the power subsystem. Whether this is true can only be determined by doing a complete statistical analysis which accounts for the weighted effects of the three error parameters (ie. 1-sigma error on inclination has a lesser effect on precession rate than 1-sigma error on non-insertion apse; however, the probabilities are equal). A preliminary analysis for ground station access during the early orbit phase is completed. Ground stations have been selected but there are several dozen other options that can be used once availability is better determined.

6 Conclusions

The orbit selected for the AEGIS satellite is a circular, sun-synchronous, dawn-dusk orbit at an altitude of 699 km. In this orbit, the satellite will experience a 3 month eclipse season and a maximum eclipse duration of approximately 20 minutes. The satellite will image at a minimum angle of elevation of 55° . At 699 km, this will allow the satellite to acquire day and night measurements of any location in Canada in a two day period and still obtain adequate coverage at the equator. The maximum distortion factor for this elevation is 1.22. The mapping error at this elevation is 2.1 km and the pointing error is 0.115° , both are determined to be adequate. The satellite will also be designed so it can successfully complete a 3 year mission with a total drift error of 17° in those three years.

7 Future Work

Much of the future work required for mission analysis has already been discussed in the body of the report. This section will summarize a few of the key items.

The orbit was not optimized once the 55° minimum imaging elevation was added. It is important to determine whether the 55° is at all flexible or if it is possible to image at lower elevations using the newest technology. Depending on the findings, it may be possible to fine tune the orbit altitude to optimize the coverage. It is likely that the changes would be very small which is good because any change will affect a variety of subsystems.

There is still a significant amount of work that can be done on launch injection errors. The analysis presented in this report is only a first iteration which was needed to provide a design point for the power subsystem. This first iteration was conservative and a full statistical analysis should be done in order to ensure that the power subsystem is not over designing.

Preliminary work has been done in the operations phase of the mission by determining ground stations to be used during the early orbit phase. Much work can still be done in this area; specifically, determining how the data from the spacecraft will be handled. This includes determining how, by who and when the data will be processed. There are also several questions unanswered in terms of how long it will require to obtain an image once it has been requested, then to downlink the data, then to process the data and finally to provide it to the client. These issues must be addressed in the future years.

References

- [1] “Classical Orbital Elements,”
http://science.nasa.gov/Realtime/rocket_sci/orbmech/state/class.html, online
- [2] Colorado Centre for Astrodynamics Research, “70x70 Earth Gravity Model,”
http://www-ccar.colorado.edu/stauch/GRAVITY_HTML/gravity.htm, online
- [3] James R. Wertz and Wiley J. Larson, “Space Mission Analysis and Design 3rd Ed.”
Kluwer Academic Publishers: California, 1999, pp144-145
- [4] V.A. Wehrle, J-P. Davignon and S. Beaudette, “Effects of Launch Injection Errors
and Atmospheric Drag on SCISAT-1 Orbit Degradation,” Proceedings of 12th CASI
Conference on Astronautics. 12-14 November 2002, Ottawa
- [5] James R. Wertz and Wiley J. Larson, “Space Mission Analysis and Design 3rd Ed.”
Kluwer Academic Publishers: California, 1999, p113
- [6] James R. Wertz and Wiley J. Larson, “Space Mission Analysis and Design 3rd Ed.”
Kluwer Academic Publishers: California, 1999, p127
- [7] “Pegasus User’s Guide,” Orbital Science Inc, Verison 5.0., August 2000

Bibliography

“Classical Orbital Elements,”

http://science.nasa.gov/Realtime/rocket_sci/orbmech/state/class.html, online.

Colorado Centre for Astrodynamic Research, “70x70 Earth Gravity Model,” http://www-ccar.colorado.edu/stauch/GRAVITY_HTML/gravity.htm, online.

D. Staley, *Spacecraft Design*, 2003.

James R. Wertz and Wiley J. Larson, “Space Mission Analysis and Design 3rd Ed.” Kluwer Academic Publishers: California, 1999.

“Pegasus User’s Guide,” Orbital Science Inc, Verison 5.0., August 2000.

“STK Online Help,” <http://www.stk.com/resources/help/help/stk44/overview.htm>, online.

V.A. Wehrle, J-P. Davignon and S. Beaudette, “Effects of Launch Injection Errors and Atmospheric Drag on SCISAT-1 Orbit Degradation,” Proceedings of 12th CASI Conference on Astronautics. 12-14 November 2002, Ottawa.

Appendix A
Angular Relationship Calculation Spreadsheet

Altitude 699 km
 Revisit Rate 2 days
 Relative
 Rotation Rate 0.004166666 deg/s
 Period 5925.473213 s
 # of passes 30

pass #	Ascending Node Relative to 0 [deg]	Difference Between Successive Nodes [deg]		
0	0		Maximum Earth Centre Angle [deg] λ	7.173726
15	10.34201658	10.34201658	Max Distance from Target [km] D	1093.29
30	20.68403316	10.34201658	Max Nadir angle [deg] n	46.76
1	24.68946777	4.005434617	Minimum Angle Elevation [deg] ϵ	36.06
16	35.03148435	10.34201658	Maximum Distortion Factor	1.698707
2	49.37893554	14.34745119		
17	59.72095212	10.34201658		
3	74.06840332	14.34745119		
18	84.41041989	10.34201658		
4	98.75787109	14.34745119		
19	109.0998877	10.34201658		
5	123.4473389	14.34745119		
20	133.7893554	10.34201658		
6	148.1368066	14.34745119		
21	158.4788232	10.34201658		
7	172.8262744	14.34745119		
22	183.168291	10.34201658		
8	197.5157422	14.34745119		
23	207.8577588	10.34201658		
9	222.2052099	14.34745119		
24	232.5472265	10.34201658		
10	246.8946777	14.34745119		
25	257.2366943	10.34201658		
11	271.5841455	14.34745119		
26	281.9261621	10.34201658		
12	296.2736133	14.34745119		
27	306.6156298	10.34201658		
13	320.963081	14.34745119		
28	331.3050976	10.34201658		
14	345.6525488	14.34745119		
29	355.9945654	10.34201658		

Appendix B
Mapping and Pointing Budget Calculation Spreadsheet

max lambda 7.1737256

Mapping Budget

Altitude[km]	Earth Centre	Distance from Target [km] D	Nadir Angle [deg] n	Elevation		azimuth error [km]	nadir angle error [km]	in-track error [km]	Cross- track error		radial error [km]	target altitude [km]	s/c clock [km]	RSS Mapping Error [km]
				Angle [deg] ε	ε				error [km]	error [km]				
699	25.6819376	3067.04	64.32	0.00	4.8242805	-136113.42	0.199687	0.1802461	0.1802461	-2291.608	-25427.54169	0.232	138487.09	
699	23.1137439	2781.25	64.19	2.70	4.3699075	103.136016	0.199718	0.1802461	0.1802461	1.9127005	21.22320546	0.232	105.41	
699	20.5455501	2496.16	63.73	5.72	3.9067563	43.7001658	0.199749	0.1802461	0.1802461	0.8994992	9.980787597	0.232	45.01	
699	17.9773563	2212.70	62.83	9.19	3.4357572	24.1741425	0.199781	0.1802461	0.1802461	0.5568947	6.17926867	0.232	25.20	
699	15.4091626	1932.30	61.29	13.30	2.9578563	14.6574697	0.199812	0.1802461	0.1802461	0.381181	4.229560753	0.232	15.55	
699	12.8409688	1657.22	58.80	18.36	2.4740136	9.18246947	0.199843	0.1802461	0.1802461	0.2715493	3.013094317	0.232	9.99	
699	10.2727751	1391.31	54.84	24.89	1.9852011	5.76979246	0.199875	0.1802461	0.1802461	0.1942499	2.15538438	0.232	6.48	
699	7.70458129	1141.74	48.50	33.80	1.4924008	3.58231904	0.199906	0.1802461	0.1802461	0.1346351	1.493902426	0.232	4.18	
699	5.13638753	922.56	38.24	46.62	0.9966025	2.21520923	0.199937	0.1802461	0.1802461	0.0851517	0.944837683	0.232	2.63	
699	2.56819376	761.10	22.06	65.38	0.4988023	1.46124903	0.199969	0.1802461	0.1802461	0.041306	0.458328539	0.232	1.65	
699	0	699.00	0.00	90.00	3.636E-08	1.21998515	0.2	0.1802461	0.1802461	2.98E-09	2.98023E-08	0.232	1.27	

Pointing Budget

Altitude[km]	Earth centre Angle	Distance from Target [km] D	Nadir Angle[deg] n	Elevation Angle		azimuth error [deg]	nadir angle error [deg]	in-track error [deg]	Cross-track error [deg]	radial error [deg]	s/c clock [deg]	RSS Pointing	
				[deg]	ε							Error [deg]	Error [deg]
699	25.6819376	3067.04	64.32	0.00	0.0901231	0.1	0.003736	0.0037362	0.0016836	0.004334025	0.1348		
699	23.1137439	2781.25	64.19	2.70	0.0900232	0.1	0.00412	0.0041201	0.0018545	0.004779365	0.1348		
699	20.5455501	2496.16	63.73	5.72	0.0896741	0.1	0.004591	0.0045907	0.0020583	0.005325234	0.1346		
699	17.9773563	2212.70	62.83	9.19	0.0896566	0.1	0.005179	0.0051788	0.0023037	0.006007417	0.1342		
699	15.4091626	1932.30	61.29	13.30	0.0877051	0.1	0.00593	0.0059303	0.0026006	0.006879163	0.1335		
699	12.8409688	1657.22	58.80	18.36	0.0855354	0.1	0.006915	0.0069147	0.0029573	0.008021056	0.1322		
699	10.2727751	1391.31	54.84	24.89	0.0817528	0.1	0.008236	0.0082362	0.0033667	0.009554017	0.1301		
699	7.70458129	1141.74	48.50	33.80	0.0748927	0.1	0.010037	0.0100365	0.0037583	0.011642392	0.1263		
699	5.13638753	922.56	38.24	46.62	0.0618942	0.1	0.012421	0.012421	0.003844	0.014408415	0.1198		
699	2.56819376	761.10	22.06	65.38	0.0375499	0.1	0.015056	0.015056	0.0028268	0.017464981	0.1103		
699	0	699.00	0.00	90.00	2.98E-09	0.1	0.016394	0.0163936	2.443E-10	0.019016625	0.1044		

Appendix C
Injection Errors Calculation Spreadsheet

	Insertion Apse	Non-Insertion Apse	Inclination
1 Sigma	5	30	0.05
3 sigma	19	90	0.15

Altitude	699 km
Inclination	98.19 deg/day
Precession rate	0.9856 deg/day
Mission Life	3 years

1-Sigma

Apogee [km]	Perigee [km]	Inclination [deg]	eccentricity	Precession Rate [deg/day]	Error in RAAN after 3 years [deg]
699	699	98.19	0	0.986399883	0.876471724
699	669	98.19	0.002124014	0.993761285	8.942727705
699	699	98.14	0	0.980418602	-5.67751735
729	699	98.19	0.002115029	0.979126001	-7.093884891
729	704	98.24	0.001761903	0.983845361	-1.922645617
729	704	98.14	0.001761903	0.971986428	-14.91707145
729	694	98.24	0.002468404	0.986281926	0.747220882
729	694	98.14	0.002468404	0.974393624	-12.2793866
704	669	98.24	0.00247714	0.998551934	14.19208195
704	669	98.14	0.00247714	0.986515733	1.003414741
694	669	98.24	0.001770639	1.001023423	16.90021524
694	669	98.14	0.001770639	0.988957431	3.678905129

3-Sigma

Apogee [km]	Perigee [km]	Inclination [deg]	eccentricity	Precession Rate [deg/day]	Error in RAAN after 3 years [deg]
699	699	98.19	0	0.986399883	0.876471724
699	609	98.19	0.006399226	1.008752471	25.36931999
699	699	98.04	0	0.968453803	-18.78794487
789	699	98.19	0.006318361	0.964835148	-22.7530868
789	718	98.34	0.004977845	0.977780076	-8.568681949
789	718	98.04	0.004977845	0.942843645	-46.85027648
789	680	98.34	0.007662458	0.987019488	1.555404171
789	680	98.04	0.007662458	0.951752929	-37.08792757
718	609	98.34	0.007739718	1.02229534	40.20891869
718	609	98.04	0.007739718	0.985768362	0.18448307
684	609	98.34	0.005338382	1.030915889	49.65488581
684	609	98.04	0.005338382	0.994080897	9.292942415

Appendix D

Lifetime due to Atmospheric Drag Sample Graph

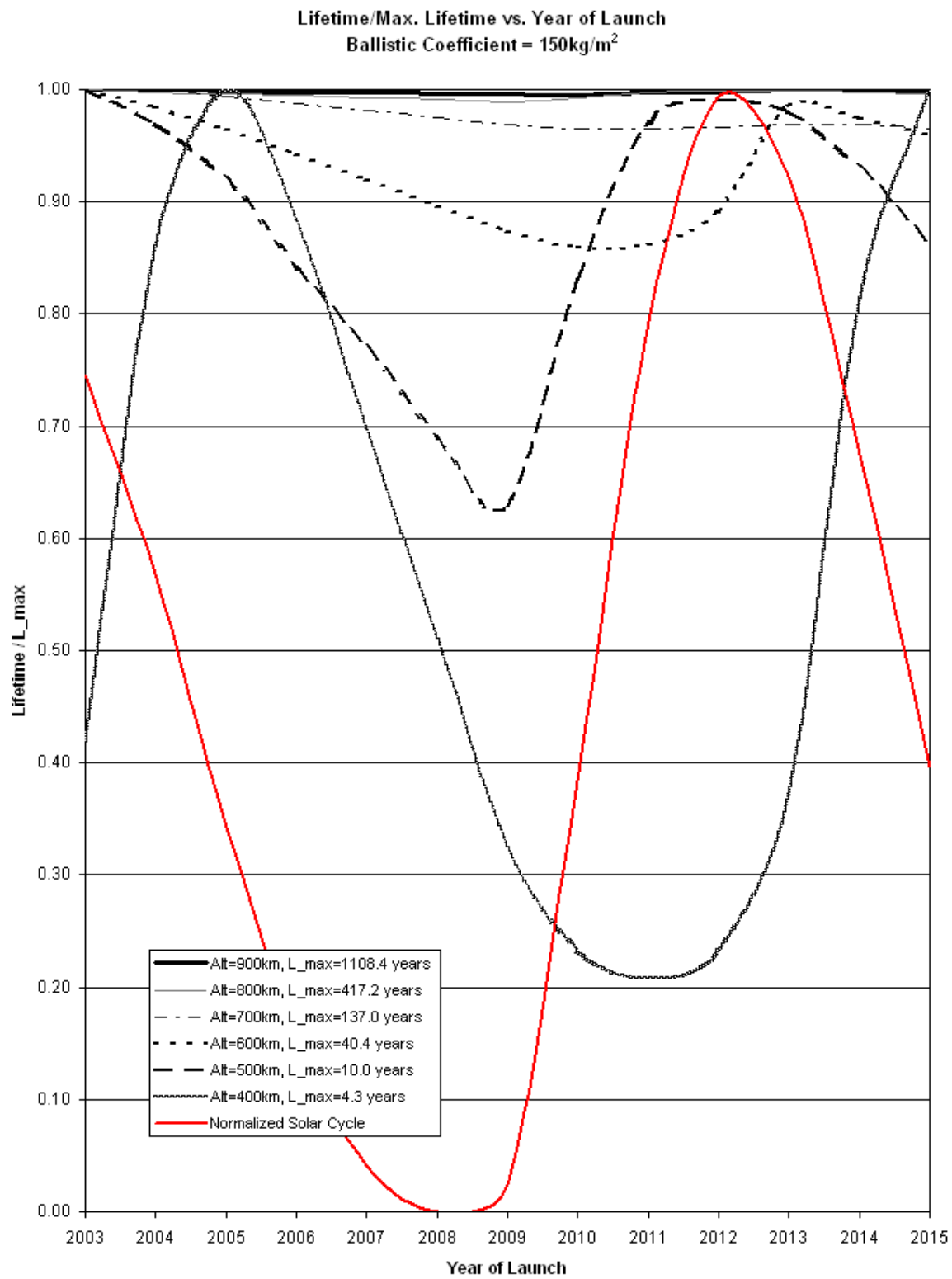


Figure D.1: Lifetime vs. Year of Launch for Ballistic Coefficient of 150kg/m^2